Supplementary Material

Unexpected Spontaneous Symmetry Breaking and Diverse Ferroicity emerged in Two-dimensional Mono-Metal Phosphorus Chalcogenides

Hou-Yi Lyu[1†], Xing-Yu Ma[2†], Kuan-Rong Hao[2], Zhen-Gang Zhu[2,3], Qing-Bo Yan[1*], Gang Su[4,2,1*]

[1]Center of Materials Science and Optoelectronics Engineering, College of Materials Science and Optoelectronic Technology, University of Chinese Academy of Sciences, Beijing 100049, China.

[2]School of Physical Sciences, University of Chinese Academy of Sciences, Beijing 100049, China.

[3]School of Electronic, Electrical and Communication Engineering, University of Chinese Academy of Sciences, Beijing 100049, China.

[4]Kavli Institute for Theoretical Sciences, and CAS Center of Excellence in Topological Quantum Computation, University of Chinese Academy of Sciences, Beijing 100190, China

[†] These authors contributed equally to this work

Email: yan@ucas.ac.cn (Q.-B. Yan)

Email: gsu@ucas.ac.cn (G. Su)

Table of Contents

1. The calculation of out-of-plane electric polarization

The total out-of-plane electric polarization per unitcell has the form of $P_{unitcell} = P_{\text{ion}} + P_{\text{el}}$, where P_{ion} and P_{el} represents the out-of-plane ion polarization and out-of-plane electron polarization, respectively. We calculate P_{ion} based on the point charge model. The out-of-plane electron polarization is calculated using $P_{\text{el}} = \iint \text{z}\rho(\vec{r})\text{d}\vec{r}$, where $\rho(\vec{r})$ is the electron density and z is the spatial position along the z direction. The electric polarization can be defined in 3D or 2D form, and the conversion equations $P_{unitcell} = P_{3D} \times V = P_{2D} \times S$, where V and S are the volume and area of unitcell, respectively. We adopt pC/m as the unit of P_{2D} in the main text.

2. The calculation of piezoelectric coefficients

Piezoelectricity is a property of electric polarization caused by macroscopic strains. The piezoelectricity of 2D materials can be described by the coupling between surface polarization (P_i), macroscopic electric field (E_i), and stress (σ_{jk}) or strain (ε_{jk}), *i.e.*, $e_{ijk} = \partial P_i / \partial \varepsilon_{jk} = \partial \sigma_{jk} / \partial E_i$ and $d_{ijk} = \partial P_i / \partial \sigma_{jk} = \partial \varepsilon_{jk} / \partial E_i$. The subscripts i, j, and $k \in \{1,2,3\}$, where 1, 2, and 3 correspond to the spatial x, y, and z directions, respectively. In the Voigt notation, e_{ijk} and d_{ijk} are reduced to e_{il} and d_{ib}, respectively, where $l \in \{1,2,\ldots,6\}$, which are correlated by elastic stiffness tensor C_{kl} as $e_{il} = d_{ik} C_{kl}$.

We adopted the methods proposed by Evan J. Reed [1] and Richard G. Hennig et. al., [2], which combines the symmetry analysis and DFT calculations to obtain the piezoelectric coefficients of 2D materials. DFT programs like VASP calculate the piezoelectric coefficients assuming periodic boundary conditions in a 3D system. To convert these coefficients to a 2D system, the above method assumes plane stress and plane strain conditions ($\varepsilon_{ij} = \sigma_{ij} = 0$ for $i = 3$ *or* $j = 3$) but the polarization is not limited to be in-plane [2], which implies that the d_{33} or e_{33} are not considered. The point group of the ferroelectric 2D MPX_3 members is 3m (C_{3v}) and the mirror symmetry is missing, which mean that they can exhibit nonzero in-plane coefficients e_{11} (d_{11}) and out-of-plane coefficients e_{31} (d_{31}).

3. The considered magnetic configurations

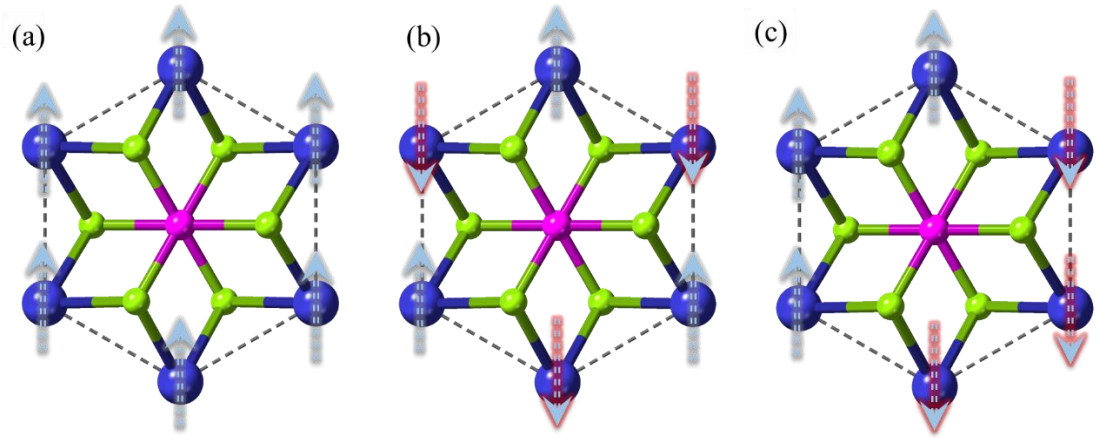

Figure S1. The considered magnetic configurations. (a) ferromagnetic and (b) Néel antiferromagnetic and (c) zigzag-antiferromagnetic configuration. Blue, purple, and green balls represent M, P, and X atoms, respectively. Blue and red arrows indicate the directions of magnetic moments. By comparing the energy of different magnetic configurations, we obtained the preferred magnetic order.

4. Phonon dispersion of 2D ferroelectric MPX_3 members

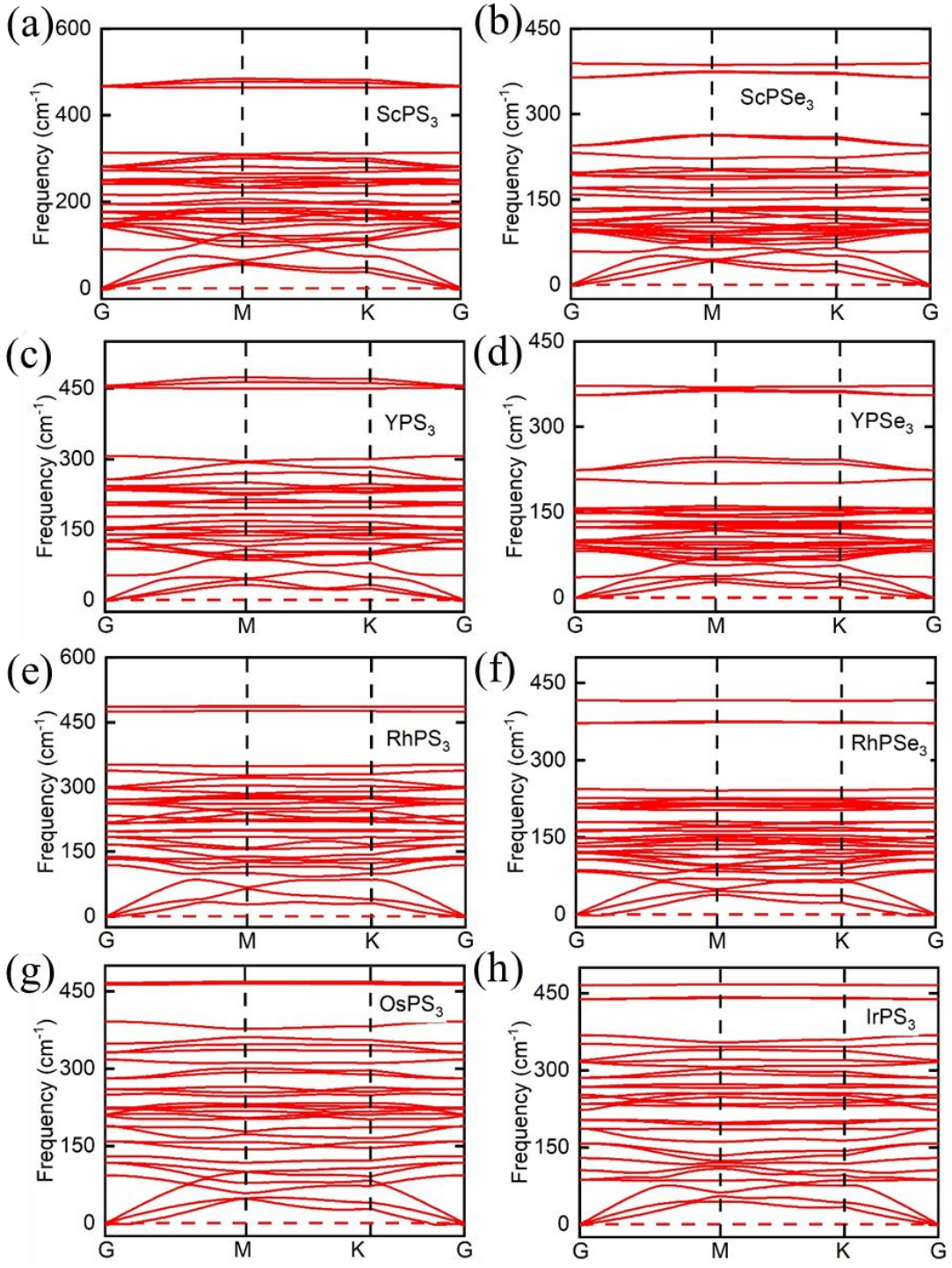

Figure S2. The phonon dispersions for 2D ferroelectric MPX_3 members.

5. Phonon dispersion of non-ferroelectric 2D MPX_3 members

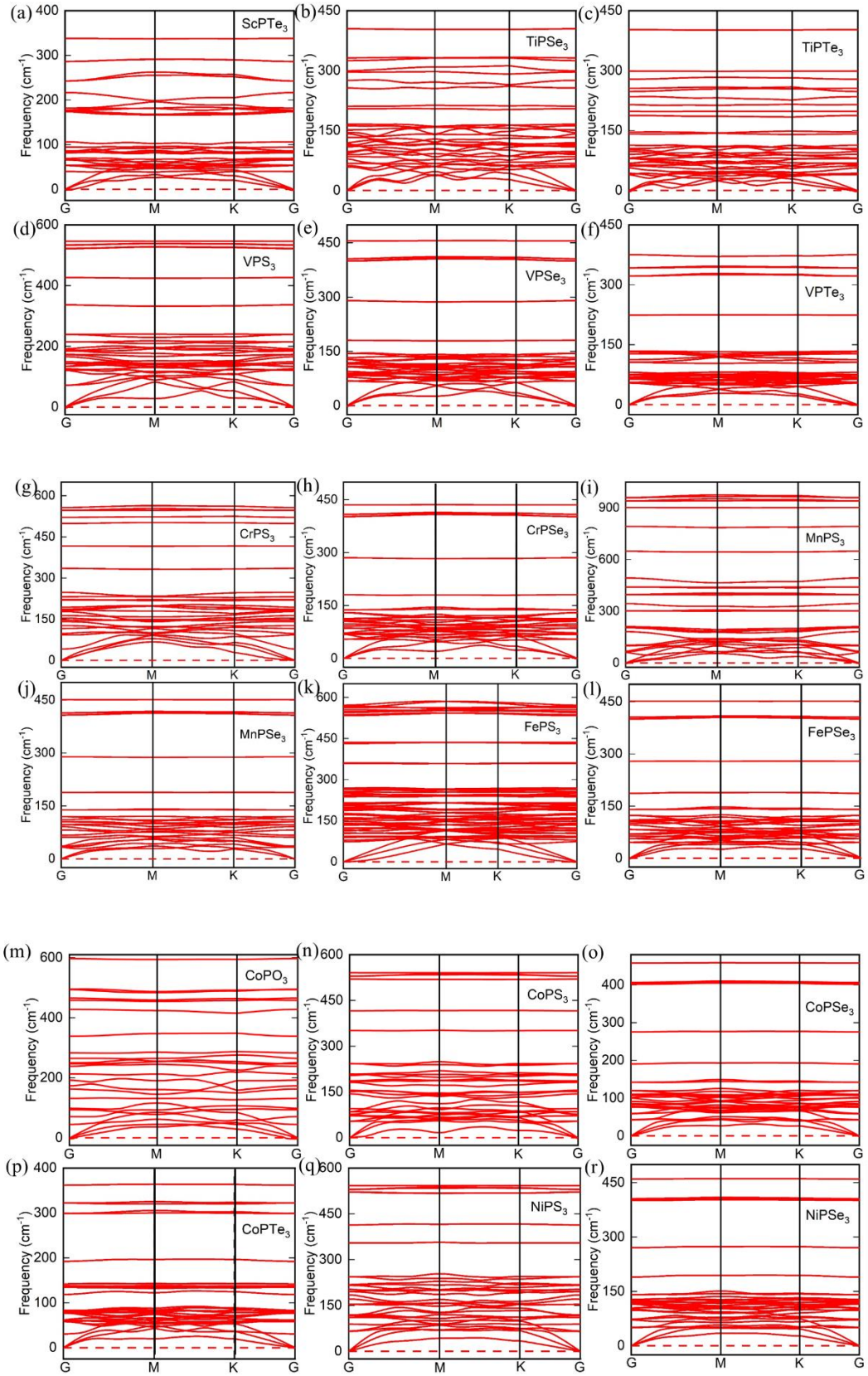

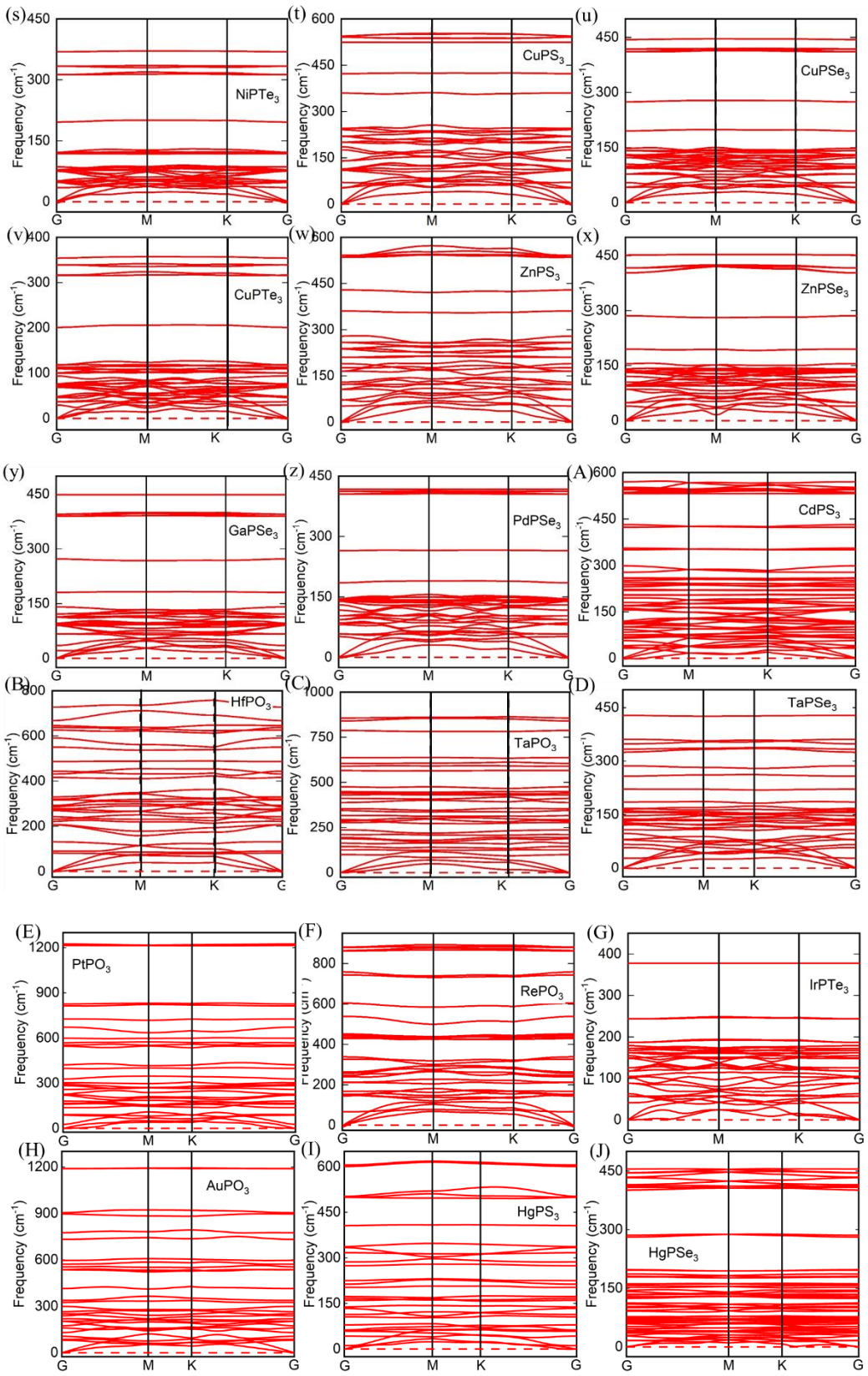
(s)
NiPTe3
(t)
CuPS3
(u)
CuPSe3
(v)
CuPTe3
(w)
ZnPS3
(x)
ZnPSe3
(y)
GaPSe3
(z)
PdPSe3
(A)
CdPS3
(B)
HfPO3
(C)
TaPO3
(D)
TaPSe3
(E)
PtPO3
(F)
RePO3
(G)
IrPTe3
(H)
AuPO3
(I)
HgPS3
(J)
HgPSe3
Frequency (cm-1)
G
M
K
G

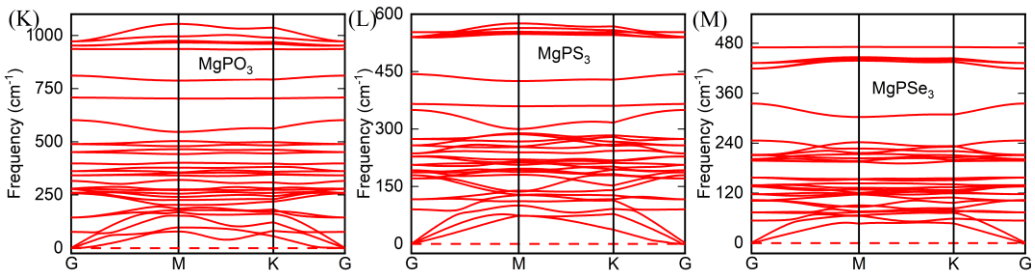

Figure S3. Phonon band structures of non-ferroelectric 2D MPX_3.

6. The thermodynamic stability of ferroelectric 2D MPX_3 members

The thermodynamic stability can be described by the heat of formation (E_f). We calculated the heat of formation of ferroelectric 2D MPX_3 members with dynamic stability. Here, the heat of formation (E_f) are obtained by using the equation $E_f = \frac{E(M_2P_2X_6)-2\times E(M)-2\times E(P)-6\times E(X)}{10}$, where $E(M_2P_2X_6)$, $E(M)$, E(P) and E(X) represent the energy of per unit cell ($M_2P_2X_6$), the average energy (per atom) of simple substance M, P and X, respectively. According to above definition, E_f <0 implies that the process forming the compound from simple substances is exothermic, and a more negative E_f indicates a better thermodynamic stability. The results are listed in Table S1. The E_f of eight ferroelectric members are negative, and most of them are ranging from -1.47 to -2.41 eV, except that of monolayer $OsPS_3$ is only -0.49 eV, indicating that most of them have good thermodynamic stability. As a comparison, the E_f of monolayer $MnPS_3$, $MnPSe_3$ and $NiPS_3$ obtained with the same method are -2.07, -1.22 and -2.18 eV, respectively. Note that their monolayer or few-layer forms had already been successfully synthesized.[3-5] Thus, these materials not only have good dynamic stability but also have good thermodynamic stability, and most of them are promising to be synthesized experimentally in future.

Table S1. The heat of formation of ferroelectric 2D MPX_3 members

Formula	E_f/atom (eV)
$Sc_2P_2S_6$	-2.24
$Sc_2P_2Se_6$	-1.47
$Y_2P_2S_6$	-2.41
$Y_2P_2Se_6$	-1.64
$Rh_2P_2S_6$	-2.41
$Rh_2P_2Se_6$	-1.73
$Os_2P_2S_6$	-0.49
$Ir_2P_2S_6$	-1.97

7. Electronic energy band of 2D ferroelectric MPX_3 members

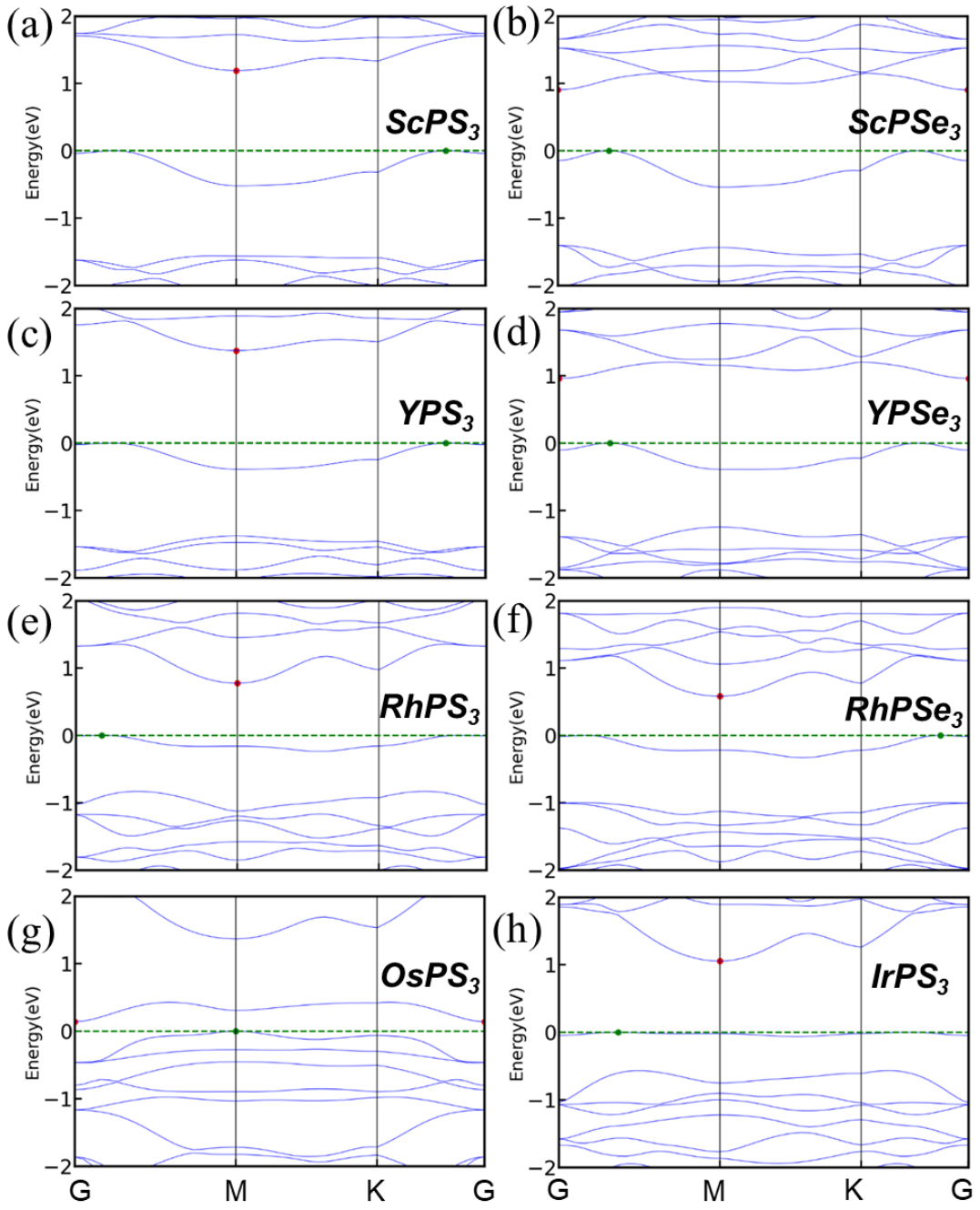

Figure S4. Electronic band structures (GGA+U) of 2D ferroelectric MPX3 members The Fermi level is set as zero.

8. Electronic energy bands of stable non-ferroelectric 2D MPX_3 members

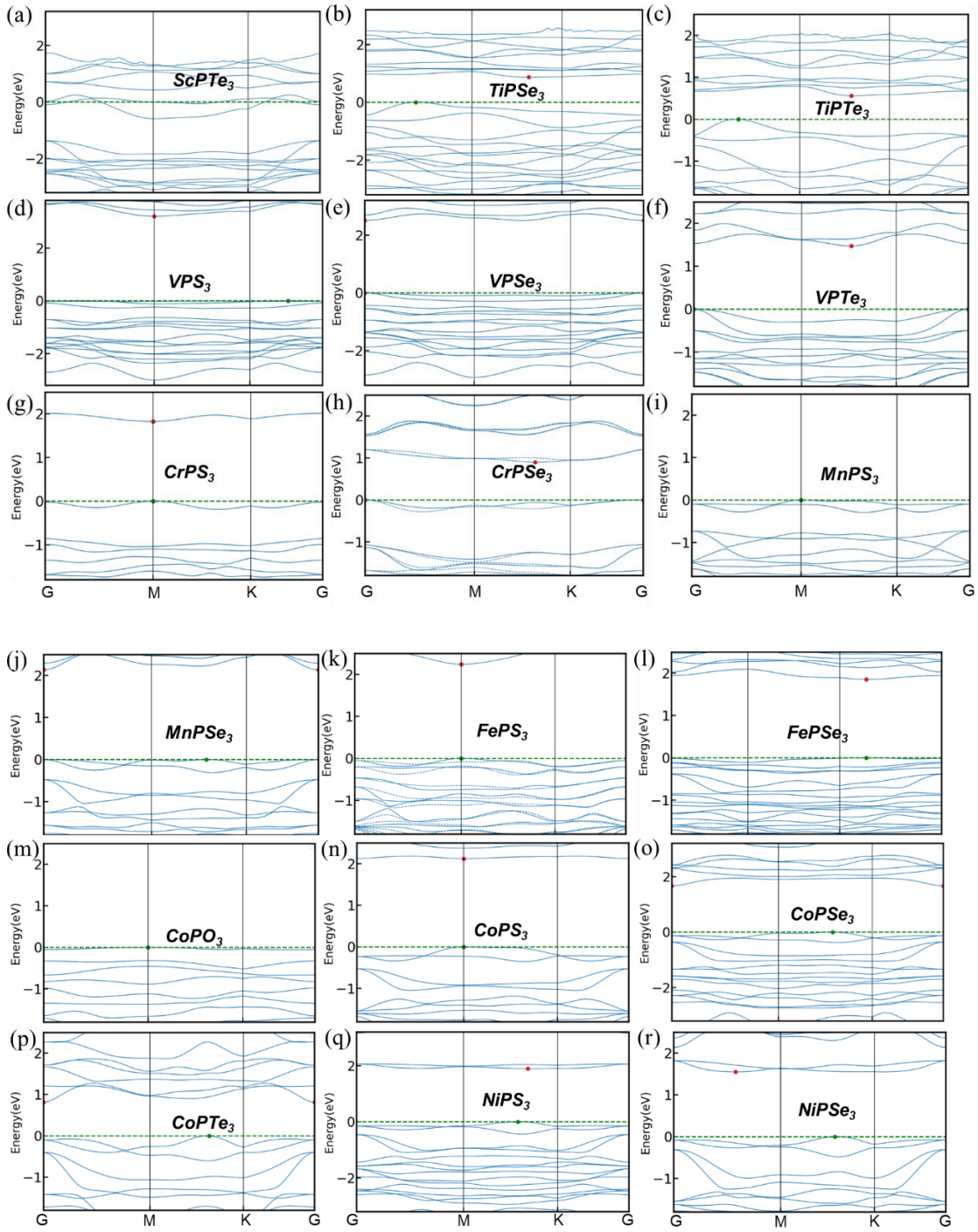

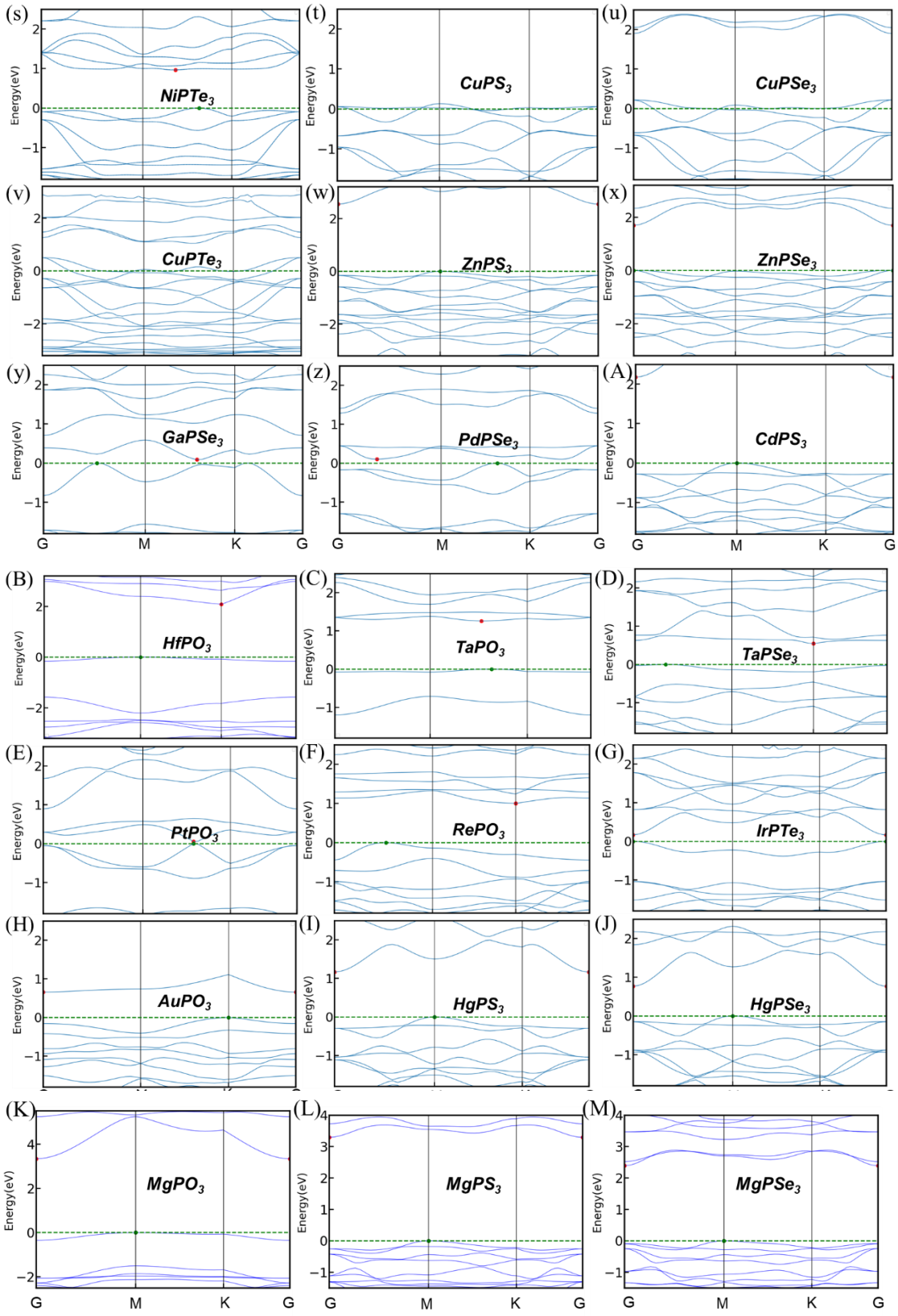

Figure S5. Electronic band structures (PBE-GGA+U) for stable 2D non-ferroelectric MPX_3. The Fermi level is set as zero.

9. The piezoelectric properteis of 2D ferroelectric MPX_3 members

Table S2. Elastic stiffness and piezoelectric coefficients of stable 2D ferroelectric MPX_3 members

Formula	C_{11} (N/m)	C_{12} (N/m)	e_{11} (10^{-10} C/m)	e_{31} (10^{-10} C/m)	Piezoelectric (d_{11}, pm/V)	Piezoelectric (d_{31}, pm/V)
$ScPS_3$	45.64	31.80	6.52	0.58	47.12	0.36
$ScPSe_3$	40.86	25.14	4.88	0.50	31.07	1.69
YPS_3	42.82	27.70	5.98	0.07	39.55	0.01
$YPSe_3$	36.38	20.93	4.56	0.04	29.48	0.01
$RhPS_3$	77.01	36.83	1.99	0.75	4.96	0.01
$RhPSe_3$	69.57	32.44	1.87	0.55	5.03	0.21
$IrPS_3$	88.26	37.81	1.97	0.72	3.90	0.50

10. The ferroelectric trantition path of 2D ferroelectric MPX_3 members

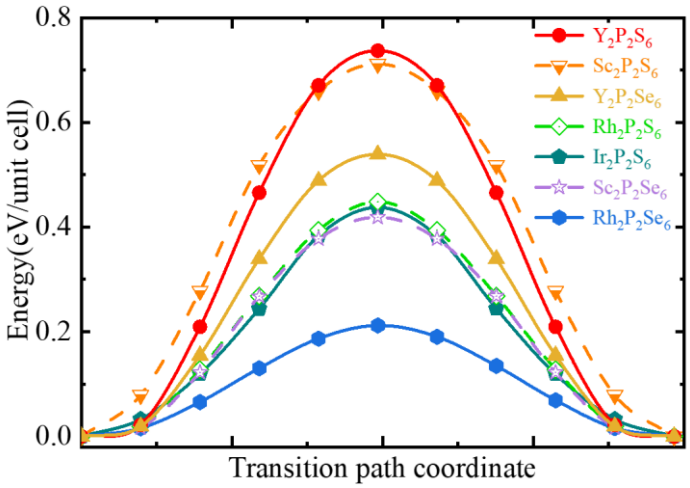

Figure S6. Ferroelectric transition barrier diagram of stable ferroelectric MPX_3 members obtained by CI-NEB calculations.

The ferroelectric trantition path of 2D ferroelectric MPX3 members are obtained by employing the CI-NEB (Climbing Image Nudged Elastic Band) method, which was developed by H. Jónsson and G. Henkelman group [6] and implemented in VTST scripts [7]. The energy barriers are listed in Table 1 of the main text.

11. Stable anti-ferromagnetic (AFM) 2D MPX_3 members

Table S3. Band gap and prefered magnetic order of stable 2D AFM MPX_3 members

Unit cell Formula	gap / eV	preferred magnetic order
$Co_2P_2O_6$	3.17	zigzag
$Co_2P_2S_6$	2.12	zigzag
$Co_2P_2Se_6$	1.67	zigzag
$Co_2P_2Te_6$	0.81	zigzag
$Cr_2P_2S_6$	1.83	Néel
$Cr_2P_2Se_6$	0.90	Néel
$Fe_2P_2S_6$	2.24	zigzag
$Fe_2P_2Se_6$	1.85	zigzag
$Mn_2P_2S_6$	2.85	Néel
$Mn_2P_2Se_6$	2.14	Néel
$Ni_2P_2S_6$	1.90	zigzag
$Ni_2P_2Se_6$	1.55	zigzag
$Ni_2P_2Te_6$	0.96	zigzag
$V_2P_2S_6$	3.20	Néel
$V_2P_2Se_6$	2.51	Néel
$V_2P_2Te_6$	1.47	Néel

References

[1] K. N. Duerloo, M. T. Ong, and E. J. Reed. Intrinsic Piezoelectricity in Two-Dimensional Materials. J. Phys. Chem. Lett. 3, 2871–2876 (2012).

[2] M. N. Blonsky, H. L. Zhuang, A. K. Singh, and R. G. Hennig. Ab Initio Prediction of Piezoelectricity in Two-Dimensional Materials. ACS Nano 9, 9885–9891 (2015).

[3] K. Kim, S. Y. Lim, J. Kim, et. al. Antiferromagnetic ordering in van der Waals 2D magnetic material $MnPS_3$ probed by Raman spectroscopy. 2D Mater. 6, 041001(2019).

[4] Z. Ni, A. V. Haglund, H. Wang, et. al. Imaging the Néel vector switching in the monolayer antiferromagnet $MnPSe_3$ with strain-controlled Ising order. Nat. Nanotechnol. 16, 782–787 (2021).

[5] C. Ho, T. Hsu and L. C. Muhimmah. The band-edge excitons observed in few-layer $NiPS_3$. npj 2D Mater. Appl. 5, 8 (2021).

[6] https://theory.cm.utexas.edu/henkelman/.

[7] https://theory.cm.utexas.edu/vtsttools/index.html